Brain Structure and Function (2019) 224:741–758
https://doi.org/10.1007/s00429-018-1805-z

ORIGINAL ARTICLE

Biphasic effect of abstinence duration following cocaine self-administration on spine morphology and plasticity-related proteins in prelimbic cortical neurons projecting to the nucleus accumbens core

B. M. Siemsen[1,2] · G. Giannotti[1] · J. A. McFaddin[2] · M. D. Scofield[1,2] · Jacqueline F. McGinty[1]

Received: 8 October 2018 / Accepted: 25 November 2018 / Published online: 29 November 2018

Abstract

Cocaine self-administration (SA) in rats dysregulates glutamatergic signaling in the prelimbic (PrL) cortex and glutamate release in the nucleus accumbens (NA) core, promoting cocaine seeking. PrL adaptations that affect relapse to drug seeking emerge during the first week of abstinence, switching from an early (2 h) hypoglutamatergic state to a later (7 days) hyperglutamatergic state. Different interventions that normalize glutamatergic signaling in PrL cortex at each timepoint are necessary to suppress relapse. We hypothesized that plasticity-related proteins that regulate glutamatergic neurotransmission as well as dendritic spine morphology would be biphasically regulated during these two phases of abstinence in PrL cortical neurons projecting to the NA core (PrL–NA core). A combinatorial viral approach was used to selectively label PrL–NA core neurons with an mCherry fluorescent reporter. Male rats underwent 2 weeks of cocaine SA or received yoked-saline infusions and were perfused either 2 h or 7 days after the final SA session. Confocal microscopy and 3D reconstruction analyses were performed for Fos and pCREB immunoreactivity (IR) in the nucleus of layer V PrL–NA core neurons and GluA1–IR and GluA2–IR in apical dendritic spines of the same neurons. Here, we show that cocaine SA decreased PrL–NA core spine head diameter, nuclear Fos–IR and pCREB–IR, and GluA1–IR and GluA2–IR in putative mushroom-type spines 2 h after the end of cocaine SA, whereas the opposite occurred following 1 week of abstinence. Our findings reveal biphasic, abstinence duration-dependent alterations in structural plasticity and relapse-related proteins in the PrL–NA core pathway after cocaine SA.

Keywords Cocaine · Prelimbic cortex · Nucleus accumbens · Dendritic spines · AMPA receptors · Glutamate

Introduction

Cocaine self-administration (SA) leads to a myriad of adaptations in plasticity-related proteins (PRPs) that mediate glutamatergic transmission in the prelimbic (PrL) cortex. These neuroadaptations change dramatically during the first week of abstinence. Two hours after cocaine exposure ends (i.e., early withdrawal), we have observed dephosphorylation of extracellular signal-regulated kinase 2 (ERK2), cAMP response-element-binding protein (CREB), GluN2A/B-containing NMDA receptors, and increased activation of STriatal-Enriched protein Tyrosine Phosphatase (STEP) (Whitfield et al. 2011; Go et al. 2016; Siemsen et al. 2018). Normalizing these dephosphorylation events with a single intra-PrL infusion of Brain-Derived Neurotrophic Factor (BDNF) or the STEP inhibitor, TC-2153, immediately after

M. D. Scofield and Jacqueline F. McGinty contributed equally to this work.

Electronic supplementary material The online version of this article (https://doi.org/10.1007/s00429-018-1805-z) contains supplementary material, which is available to authorized users.

✉ Jacqueline F. McGinty
mcginty@musc.edu

[1] Department of Neuroscience, Medical University of South Carolina, 173 Ashley Avenue MSC 510, Charleston, SC 29425, USA

[2] Department of Anesthesiology and Perioperative Medicine, Medical University of South Carolina, 167 Ashley Avenue, Charleston, SC 29425, USA

SA provides an enduring decrease in relapse (Whitfield et al. 2011; Go et al. 2016; Siemsen et al. 2018; Berglind et al. 2007) and normalizes dysfunctional glutamate release in the nucleus accumbens (NA) core (Berglind et al. 2009). In contrast, after 1 week of abstinence (i.e., early abstinence) from cocaine SA, a hyper-phosphorylation of the cAMP-dependent protein kinase A (PKA) targets, CREB^{S133} and GluA1^{S845}, in the PrL cortex and synapsin-I^{S9} in the NA core emerge (Sun et al. 2014b, a). Inhibition of PKA with intra-PrL Rp-cAMPs, but not BDNF, at this timepoint prevents context-induced relapse to cocaine seeking by normalizing these adaptations (Sun et al. 2014a).

These findings indicate that biphasic alterations in glutamatergic transmission in the PrL cortex occur during early withdrawal and abstinence, requiring different time-dependent interventions to decrease drug seeking. However, it is unknown whether the global changes in PrL PRPs are expressed by pathway-specific projections to subcortical targets or if the changes in the expression of synaptic PRPs (AMPA receptors) are associated with morphometric alterations in dendritic spines that have previously been linked to relapse propensity (Gipson et al. 2013; Russo et al. 2010).

Changes in dendritic spine morphology and AMPA receptor expression in spine heads are associated with alterations in glutamatergic transmission. For example, GluA1^{S845} phosphorylation enhances glutamate currents by promoting the membrane insertion of AMPA receptors (Banke et al. 2000). Furthermore, GluA1-containing AMPA receptors are preferentially incorporated into mushroom-type dendritic spines that stabilize synapses following learning (Matsuo et al. 2008) and AMPA receptor-mediated currents are augmented in mushroom-type spines, relative to smaller spines, in response to glutamate uncaging (Matsuzaki et al. 2001). Thus, cocaine-induced adaptations in glutamate transmission are likely associated with altered dendritic spine morphology and AMPA receptor expression in spine heads.

Although cocaine-induced adaptations in structural plasticity within the NA core are well-documented (Gipson et al. 2013; Stefanik et al. 2016; Spencer et al. 2017; Toda et al. 2010), conflicting findings have been reported concerning modifications in structural plasticity in PrL pyramidal neurons following abstinence from cocaine SA. Golgi staining studies have demonstrated elevated apical spine density on layer V PrL neurons after 1 month of abstinence (Robinson et al. 2001) and increased basal spine density on layer V PrL neurons after 1 week of abstinence (Rasakham et al. 2014). Recently, dye-filling techniques and higher resolution imaging studies have shown that after 2 weeks of abstinence from cocaine SA, global PrL apical spine density (i.e., layer II/III and V) is reduced, but is accompanied by an increase in spine volume (Radley et al. 2015). Collectively, these data demonstrate that changes in structural plasticity in the PrL cortex after cocaine SA depend on the type of pyramidal neurons analyzed, the duration of abstinence, and perhaps most importantly, the technological strategy used to measure dendritic spine morphology.

However, it is now accepted that PrL neurons projecting to distinct subcortical targets display heterogeneity regarding the encoding of reward-associated stimuli (Otis et al. 2017; Giannotti et al. 2018). Accordingly, to achieve cell type and projection specificity, viral vectors and Cre-dependent fluorescent reporters have recently been used to label neurons for spine analyses in the nucleus accumbens (Dos Santos et al. 2017; Barrientos et al. 2018) and the PrL cortex (Barrientos et al. 2018). Recently, we found that a combinatorial viral approach fully labels pyramidal neurons in the PrL cortex with pathway specificity that can be combined with immunohistochemical detection of AMPA receptors in different dendritic subcompartments, allowing for analysis of dendritic spine morphology and associated protein expression in PrL cortical neurons projecting to the NA core (PrL–NA core). In the current study, we focused our attention specifically on the distal apical tuft of layer V PrL–NA core neurons, because chronic stress produces a specific reduction in distal apical tuft spine density in layer V PrL cortical neurons (Liu and Aghajanian 2008) and recent evidence indicates a relationship between abstinence from cocaine SA, stress, and decreased PrL cortical apical dendrite spine density (Radley et al. 2015). Moreover, the distal apical tuft represents an important layer V pyramidal neuron subcompartment for NMDA receptor and Ca^{2+} spike generation mediating synaptic integration and dendritic summation (Larkum et al. 2009). Thus, structural modifications in the distal tuft may directly impact PrL–NA core neuronal physiology.

Given that PrL glutamatergic transmission switches from a putatively hypoactive to a hyperactive state as a function of the duration of abstinence from cocaine SA (Dennis et al. 2018; Sepulveda-Orengo et al. 2017), we hypothesized that nuclear (Fos, pCREB) and dendritic (GluA1, GluA2) PRPs and dendritic spine morphometric features would follow a similar trajectory in PrL–NA core neurons, since pathological adaptations that promote cocaine seeking occur within this pathway (Kalivas et al. 2005; Kalivas 2009; Chen et al. 2013).

Materials and methods

Rats

Thirty-two adult male Sprague Dawley rats were used in this study (Charles Rivers Laboratories; Wilmington, MA, USA). All rats weighed 275–325 g at the time of surgery. Rats were individually housed on a 12 h reverse light/dark cycle (lights on at 6 AM). Upon arrival, rats were allowed at least 3 days of acclimation to the vivarium. During this time,

they were provided standard rat chow (Harlan; Indianapolis, IN, USA) and water ad libitum. All animal use protocols were approved by the Institutional Animal Care and Use Committee of the Medical University of South Carolina and were performed according to the National Institutes of Health Guide for the Care and Use of Laboratory Animals (8th ed. 2011).

Viral constructs and surgery

On the day of surgery, rats were injected i.p. with a ketamine (66 mg/kg) and xylazine (1.33 mg/kg) mixture for anesthesia and ketorolac (2.0 mg/kg) for analgesia prior to undergoing silastic catheter (Fisher Scientific; Hampton, NH) implantation in the right jugular vein. Following catheterization, rats were secured in a stereotaxic apparatus (Kopf Instruments, Tujunga, CA, USA) for intra-cranial virus microinjections.

All viral procedures and constructs used in this study were approved by the Medical University of South Carolina Institutional Biosafety Committee. All rats received a single microinjection (0.75 µl/hemisphere) of a Canine adeno virus type 2 expressing a Cre-eGFP (CAV2-Cre-eGFP) fusion protein under the control of a CMV promoter (3.6×10^{12} vg/ml) obtained from the Montpellier vector core (Montpellier, FR) within the NA core (coordinates: + 1.6 mm AP from bregma, ± 2.8 mm ML from bregma, − 7.1 mm DV from skull, 10° angle). Rats were then microinjected within the prelimbic cortex (coordinates: + 2.8 mm AP from bregma, ± 0.6 mm from bregma, − 3.8 DV from skull) with an AAV5–hSyn–DIO–mCherry (~ 1.5×10^{12} vg/ml) obtained from Addgene (Cambridge, MA, USA). Injections were performed over a period of 5 min (0.15 µl/min) using a Nanoject II (Drummond scientific, Broomall, PA, USA) and injectors were left in place for 10 min to facilitate diffusion away from the injection site, then slowly retracted. Following surgery, bore holes were sealed with dental acrylic, and the incision was sutured closed. Rats were allowed at least 5 days of recovery, during which food and water were available ad libitum prior to beginning behavioral training.

Drug self-administration

Rats underwent cocaine self-administration or received yoked-saline infusions for 12–14 days (2 h/day, criterion of ≥ 10 infusions/day) on an FR1 schedule of reinforcement. Self-administration was conducted in the standard Med Associates operant chambers (Fairfax, VT, USA) containing two retractable levers. Active lever presses elicited a light + tone conditioned-cue complex followed by a single bolus (200 µg/50 µl) of cocaine hydrochloride (NIDA, Research Triangle Park, NC, USA), followed by a 20 s timeout period during which active lever presses had no programmed consequence. Inactive lever presses had no programmed consequence, but were recorded. Yoked-saline controls received a single non-contingent bolus of 0.9% sterile saline (with light and tone cues) when their yoked partner received a contingent cocaine infusion.

Abstinence duration and perfusions

In Experiment 1, rats were returned to their homecage for 2 h after the final cocaine SA session, heavily anesthetized with equithesin (~ 0.5 ml, i.v.), and transcardially perfused with 150 ml of ice-cold 0.1 M phosphate buffer (PB) at 60 ml/min followed by 200 ml of ice-cold 4% paraformaldehyde (PFA, pH 7.4) in 0.1 M PB. Brains were rapidly removed and immersed in the same fixative for 1 h, then transferred to a 20% sucrose solution and kept at 4 °C prior to sectioning. In Experiment 2, rats were perfused 1 week after the final cocaine SA session following forced homecage abstinence, where food and water were provided ad libitum, and brains were post-fixed for 24 h. To match virus expression duration between experiments, rats in experiment 1 were given an extra week of recovery after surgery prior to beginning SA.

Immunohistochemistry

Coronal sections (AP + 2.52–4.2 mm from bregma) were sliced at 80 µm using a Leica cryostat and collected in 0.1M PBS containing 0.01% sodium azide. Sections were stored at 4 °C until immunohistochemical processing. Immunohistochemistry was performed according to previously published protocols (Scofield et al. 2016). Briefly, sections were blocked with 0.1 M phosphate-buffered saline containing 2% Triton X-100 (PBST) and 2% normal goat serum (NGS) for 2 h at room temperature (RT). Sections were then incubated in chicken anti-mCherry (1:2000; LS Biosciences #LS-C204825, Seattle, WA RRID:AB_2716246), mouse anti-GluR2 (2.13 µg/ml; Millipore #MAB397, Billerica, MA RRID:AB_2113875), rabbit anti-GluA1 (1:500; Cell Signaling Technology #13185, Danvers, MA, USA), rabbit anti-Fos (1:1000, Santa Cruz Biotechnology #sc-52, Dallas, TX RRID:AB_2106783), or mouse anti-pCREB^{S133} (1:200, Cell Signaling Technology, #9196, Danvers, MA RRID:AB_331275) at 4 °C overnight. Sections were washed 3 × 10 min in PBST, and then incubated with species-appropriate Alexa Fluor®594 (mCherry), Alexa Fluor®488 (Fos, pCREB), or Alexa Fluor®647 (GluA1, GluA2)-conjugated secondary antisera (1:1000, Abcam, Cambridge, UK) diluted in 2% PBST with 2% NGS for 5 h at RT protected from light. Sections were washed 3 × 10 min and then mounted on superfrost plus slides using ProLong® gold Antifade (Thermo Fisher Scientific; Waltham, MA). Slides were stored at 4 °C until imaging.

Confocal microscopy

Fos/pCREB quantitation

Confocal Z-stack (50 µm) images were captured with a Leica SP8 confocal microscope. Fos or pCREB immunoreactivity was excited using an Optically Pumped Semiconductor Laser (OPSL) 488 nm laser line using a 20× air objective. mCherry–IR was excited using an OPSL 552 nm laser line. Z-stacks were then imported to Imaris. The spot tool in Imaris was used, and detection threshold and spot size were empirically determined and maintained constant for each measurement. The number of pCREB–IR or Fos–IR cells was counted automatically for each hemisphere and averaged across 1 section per rat. The spots colocalization extension in Imaris was used to determine coregistry between $mCherry^+$ and $Fos/pCREB^+$ somas. The number of mCherry–IR neurons that are pCREB or Fos–IR was normalized to the number of total mCherry–IR neurons and expressed as a percentage of total mCherry–IR neurons.

Dendritic spine imaging

Confocal Z-series data sets were acquired using a Leica SP8 laser-scanning confocal microscope (Wetzlar, Germany). Dendrites selected for imaging had the following characteristics: (1) the apical dendritic segment (typically 40–50 µm in length) was visually connected to the cell body of origin; (2) the dendrite selected was after the third branch point; (3) was > 15 µm below the surface of the tissue; and (4) was located within 10 µm of the end of the dendrite (i.e., approaching the pial surface). Overall imaging parameters including laser power, gain, pinhole, and optical section thickness were set empirically prior to imaging and were held constant for the remainder of the experiment. mCherry was excited using an OPSL 552 nm laser line, and GluA1/2 were excited using a diode 638 nm laser line. Emitted photons were collected using high-sensitivity hybrid detectors (HyD). Images were acquired using a 63× oil immersion objective (1.4 N.A.) with a 1024 × 512 frame size, 3.5× digital zoom, 700 Hz acquisition rate, and 0.1 µm step size generating a voxel size of 52 nm × 52 nm × 100 nm. Images were acquired using sub airy unit pinhole sizes. These parameters were selected to obtain optimal deconvolution as recommended by Huygens essential deconvolution software (Hilversum, The Netherlands). The resulting set of parameters allows for a minimum resolution of 150 nm XY by 300 nm Z in our reconstructions. One dendritic spine segment was imaged per neuron each with an accompanying GluA1 or GluA2 channel collected.

Imaris 3D reconstruction, morphological analyses, and colocalization

Following deconvolution, Z-stacks were imported into Bit-Plane Imaris (Zurich, Switzerland, version 9.0) for morphological analyses. Z-stacks were cropped in 3D to isolate individual dendrites, and a 3D space-filling model was generated to isolate voxels corresponding to the mCherry-positive dendrite of interest. The filament module was used to semi-manually trace identified dendritic spines as described previously (Trantham-Davidson et al. 2017). Dendritic spine head diameter was calculated using an automated threshold set by Imaris. To calculate dendritic spine density, the number of spines was normalized to the length of the dendrite (in µm).

The "create channel" filament extension was used to generate a channel defined by the filament built by Imaris, which was used for colocalization analyses. To isolate GluA1/2 IR corresponding to dendritic spine heads relative to total dendrite, the "filament analysis" extension was used to mask all GluA1/2 IR not corresponding to Imaris-defined dendritic spine heads and shafts. Filament analysis uses the predefined boundaries of the spine heads relative to the dendritic shaft to isolate specific channels of interest in dendritic subcompartments.

For colocalization analyses, a region of interest (ROI) containing only the mCherry dendrite was used. The colocalization module of Imaris was used to perform standard intensity-based colocalization analyses between total mCherry signal and total GluA1/2 signal (dendrite shaft and spine heads). The intensity value at which a voxel could be considered coregistered was set empirically by a blind investigator for both channels as described previously (Scofield et al. 2016). We recorded the percent of signal above threshold to determine whether differences in the intensity of signal impacted coregistry analyses for GluA1, GluA2, and mCherry. Percent colocalization was calculated by normalizing the total volume of GluA1/2-mCherry coregistry to the total volume of mCherry. The total colocalization channel was then separated into Imaris-defined spine heads and dendritic shaft using the "filament analysis" extension, and a 3D space-filling model was generated corresponding to colocalized voxels for (a) spine head-specific colocalization and (b) dendritic shaft-specific colocalization. Electron microscopy studies indicate that a significant amount of GluA2 expression is present in both dendritic shafts and spine heads (Vissavajjhala et al. 1996) and in vitro experiments indicate similar patterns for GluA1 (Szepesi et al. 2014). Thus, percent colocalization was determined for total GluA1/2, spine head-specific GluA1/2, and dendritic shaft-specific GluA1/2 by normalizing the volume of colocalized voxels in each compartment to the volume of the mCherry dendrite. To determine specific spine head bins that may account for overall alterations in spine head diameter, the number of

spines within each bin was normalized to the total number of spines and compared between groups. To determine spine head bins that show more/less GluA1/2 coregistry in spine heads, the volume of coregistry was manually counted in each spine, then averaged for each bin for each dendritic segment, then across segments for each animal. In a minority of instances when sections from individual animals showed mCherry neurons labeled in one for GluA1 but not GluA2, and vice versa, the spine morphometry data for that animal consisted of the run in which mCherry neurons were labeled, but the colocalization data for that animal for that specific protein probed were not included. All analyses were performed by an individual blind to experimental groups.

Statistical analyses

Behavioral data were analyzed with a two-way repeated measures (RM) ANOVA with treatment (cocaine versus saline) as a between-subjects factor and SA session as a within-subjects factor followed by Bonferroni-corrected pairwise comparisons when a significant interaction was observed. A two-tailed *t* test with or without Welch's correction was used when two groups were compared for a single dependent variable. Binned dendritic spine head and GluA1/2 colocalization volume data were analyzed with a two-way RM ANOVA with treatment (cocaine versus saline) as a between-subjects factor and bin as a within-subjects factor followed by a Bonferroni-corrected pairwise comparison test when a significant interaction was observed, as previously performed (Ball et al. 2009). Each animal's dendritic spine or colocalization data points were derived from an average across the analyzed segments. Cumulative frequency distribution data were analyzed to determine general shifts in spine head diameter for each group using a Kolmogorov–Smirnov non-parametric test when correlating spine head diameter and density with pCREB–IR Pearson's correlation test was used. Statistical outliers were detected with Grubbs' test and were excluded from all analyses, as discussed in "Results". Sample sizes for each group for each experiment are stated in the respective figure legends. Data are expressed as the mean ± SEM, and significance was determined at $p < 0.05$.

Results

Experimental design and cocaine SA

The design and timeline for Experiments 1 and 2 are shown in Fig. 1a. In Experiment 1, 16 rats underwent cocaine SA

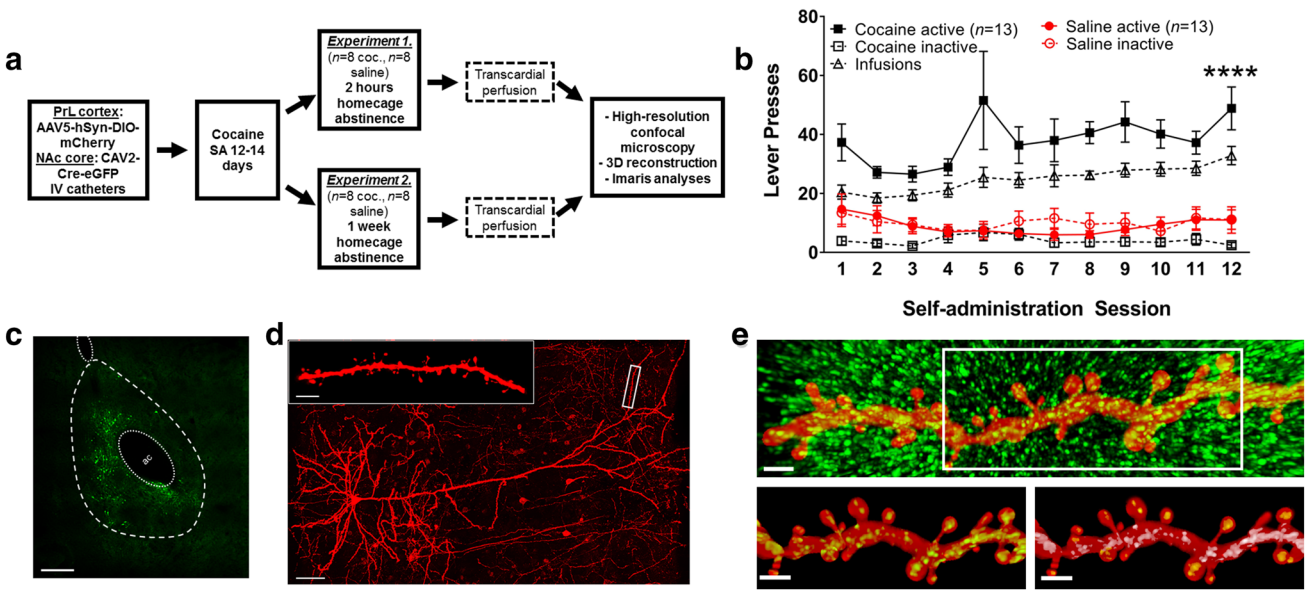

Fig. 1 Experimental timeline, virus expression, and cocaine SA data. **a** Experimental timeline for Experiments 1 and 2. **b** Cocaine SA data over the last 12 days of SA. Solid lines and closed symbols indicate active lever presses and dotted lines with open symbols indicate inactive lever presses. **c** Representative CAV2-Cre-eGFP virus expression in the NA core. Dotted lines indicate lateral ventricle (top), anterior commissure (ac, center), and border of NA core and NA shell. **d** Representative mCherry-labeled PrL–NA core layer V neuron. Inset corresponds to a representative dendritic spine segment taken from the distal apical tuft. **e** Representative mCherry-labeled spine segment from distal apical tuft of a layer V PrL–NA core neuron displaying GluA2 IR (top). Bottom left—GluA2 IR corresponding only to mCherry signal within the dendrite. Bottom right—GluA2-mCherry coregistered voxels in dendritic spine heads (yellow) and dendritic shaft (white). Scale bars indicate 200 µm (**b**), 50 µm (**c**), 5 µm (inset, **c**), 2 µm (**d**), ****$p < 0.0001$ comparing cocaine to saline active lever presses, two-way RM ANOVA, Bonferroni-corrected pairwise comparison. *SA* self-administration, d_H spine head diameter

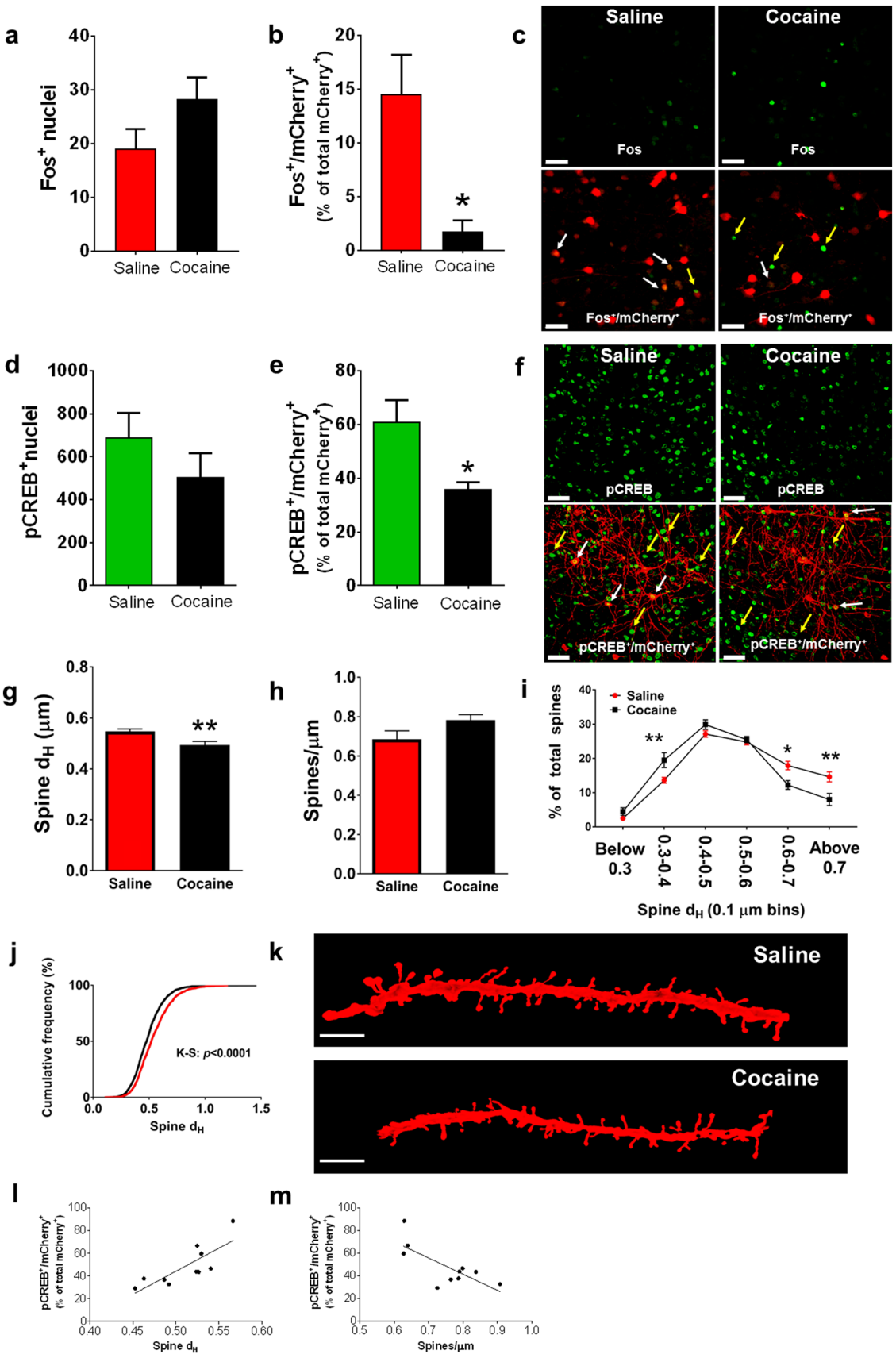
a
Fos+ nuclei
Saline
Cocaine
b
Fos+/mCherry+ (% of total mCherry+)
*
c
Saline
Cocaine
Fos
Fos+/mCherry+
d
pCREB+nuclei
e
pCREB+/mCherry+ (% of total mCherry+)
f
pCREB
pCREB+/mCherry+
g
Spine dH (μm)
**
h
Spines/μm
i
% of total spines
Below 0.3
0.3-0.4
0.4-0.5
0.5-0.6
0.6-0.7
Above 0.7
Spine dH (0.1 μm bins)
j
Cumulative frequency (%)
K-S: p<0.0001
Spine dH
k
l
m
Spines/μm

◂**Fig. 2** Cocaine SA decreased PrL–NA core Fos–IR, pCREB–IR, and dendritic spine head diameter during early withdrawal. Fos^+ nuclei in layer V of the PrL cortex (**a**) and $Fos^+/mCherry^+$ normalized to total $mCherry^+$ cells (**b**). **c** Top—representative images of Fos^+ nuclei in saline and cocaine SA rats. Bottom—representative $Fos^{+}/mCherry^+$ and $Fos^+/mCherry^-$ neurons in saline and cocaine SA rats. White arrows indicate $Fos^+/mCherry^+$ neurons, and yellow arrows indicate $Fos^+/mCherry^-$ neurons. $pCREB^+$ cells in layer V of the PrL cortex (**d**) and normalized to total $mCherry^+$ cells (**e**). **f** Top-representative images of $pCREB^+$ neurons in saline and cocaine SA rats. Bottom—representative $pCREB^+/mCherry^+$ and $pCREB^+/mCherry^-$ neurons in saline and cocaine SA rats. White arrows indicate $pCREB^+/mCherry^+$ neurons, and yellow arrows indicate $pCREB^+/mCherry^-$ neurons. **g** Cocaine SA decreased spine head diameter in cocaine SA rats compared to yoked-saline controls. **h** There was no difference in spine density between groups. Cocaine self-administering animals show a general leftward shift in percent of total spines as a function of spine head diameter (d_H) (**i**) and cumulative frequency (**j**). **k** Representative dendrites from saline (top) and cocaine SA (bottom) rats. The percentage of $pCREB^+/mCherry^+$ neurons positively correlated with dendritic spine d_H (**l**), but negatively correlated with dendritic spine density (**m**). $^*p<0.05$, $^{**}p<0.01$ compared to saline. **a, b, g, h** Two-tailed Welch's-corrected *t* test. **d, e** Two-tailed *t* test. **i** Two-way RM ANOVA with Bonferroni-corrected pairwise comparison. Scale bars indicate 40 µm (**c, f**), 5 µm (**k**). **a–c** $n=4$ per group. **d–f, l, m** $n=5$ per group. **g–k** $n=7$ (saline), $n=6$ (cocaine)

or received yoked-saline infusions and were perfused 2 h after the final session. One yoked-saline rat was excluded due to a missed NA core placement. Two cocaine animals were excluded due to failed catheters. In Experiment 2, 16 rats underwent 12–14 days of cocaine SA or received yoked-saline infusions. One yoked-saline rat did not finish the experiment due to stress reactions when handled and another was removed from analyses due to insufficient virus expression. One cocaine SA rat was removed as a statistical outlier in colocalization analyses. Figure 1b shows yoked-saline and cocaine SA lever press and infusion data. When analyzing active lever presses, there was a significant drug (cocaine versus saline) by session interaction [$F_{(11,264)}=2.01$, $p=0.02$]. Cocaine SA rats showed lever discrimination, as evidenced by a significant main effect of lever [active versus inactive, $F_{(1,24)}=60.38$, $p<0.0001$] and they pressed the active lever significantly more than yoked-saline controls in sessions 4–12 ($p<0.05$). Representative CAV2-Cre-eGFP expression in the NA core and an mCherry-expressing PrL–NA core neuron are shown in Fig. 1c, d, respectively. A representative PrL–NA core neuronal spine segment processed for GluA2–IR is shown in Fig. 1e.

Effect of cocaine SA on PrL–NA core spine morphometric features and PRPs during early withdrawal

In Experiment 1, rats underwent cocaine SA or received yoked-saline infusions and were perfused 2 h after the final session. First, we examined Fos–IR in layer V PrL cortex in a subset of sections. Early withdrawal from cocaine SA had no significant impact on global PrL Fos–IR [$t_{(6)}=1.70$, $p=0.14$, Fig. 2a]. However, we found a significant cocaine-induced reduction in Fos–IR [$t_{(6)}=3.31$, $p=0.02$, Fig. 2b] when the analysis was limited only to PrL–NA core ($mCherry^+$) neurons. Representative images are shown in Fig. 2c.

Next, a subset of tissue sections was used to analyze pCREB–IR in the PrL cortex. Early withdrawal from cocaine SA had no significant effect on global PrL pCREB–IR [$t_{(8)}=1.16$, $p=0.28$, Fig. 2d]. However, there was a significant decrease in the percentage of PrL–NA core neurons that expressed pCREB–IR [$t_{(4.7)}=2.94$, $p=0.03$, Fig. 2e]. Representative images are shown in Fig. 2f. Importantly, there was no significant difference in pCREB signal intensity between groups in the PrL cortex overall or specifically in PrL–NA core neurons, as shown in Fig. S2a, b, respectively, indicating that differences in signal intensity are unlikely to be the cause of the observed effect of cocaine.

We hypothesized that alterations in PrL–NA core PRPs during early withdrawal are associated with altered dendritic spine morphometric features and AMPA receptor expression. To address this hypothesis, we analyzed 52 dendritic segments (1651 total spines) from 7 yoked-saline rats and 54 dendritic segments (2159 total spines) from 6 cocaine SA rats. From these 13 rats, we sampled an average of 8.07 ± 2.32 (range 4–12) dendritic segments per rat. We observed a significant decrease in spine head diameter (d_H) in PrL–NA core neurons in cocaine SA rats compared to yoked-saline controls [$t_{(11)}=3.19$, $p=0.009$, Fig. 2g], yet we did not observe any significant difference in spine density [$t_{(11)}=1.83$, $p=0.09$, Fig. 2h]. Importantly, we did not observe significant differences between groups in the average spine terminal point intensity (Fig. S3a), indicating that differences in mCherry signal intensity are unlikely to contribute to the effects observed on spine d_H.

There was a significant interaction of drug and spine d_H when analyzing the percent of total spines as a function of spine d_H [$F_{(5,55)}=6.59$, $p<0.0001$]. Specifically, cocaine SA rats displayed a significant increase in the percentage of total spines with head diameters between 0.3 and 0.4 µm ($p=0.008$) and a significant decrease in the percentage of total spines with head diameters between 0.6 and 0.7 µm ($p=0.01$) and above 0.7 µm ($p=0.002$, Fig. 2i). These changes were associated with a leftward shift in spine d_H when analyzing all spines in yoked saline and cocaine SA rats (K–S $D=0.14$, $p<0.0001$, Fig. 2j). Representative dendritic images are shown in Fig. 2k. Intriguingly, there was a positive correlation between spine d_H and pCREB–IR ($r^2=0.64$, $p=0.005$, Fig. 2l), but a negative correlation between spine density and pCREB–IR ($r^2=0.44$, $p=0.01$, Fig. 2m). However, no such correlations existed between spine d_H and Fos–IR nor spine density and Fos–IR (data not shown).

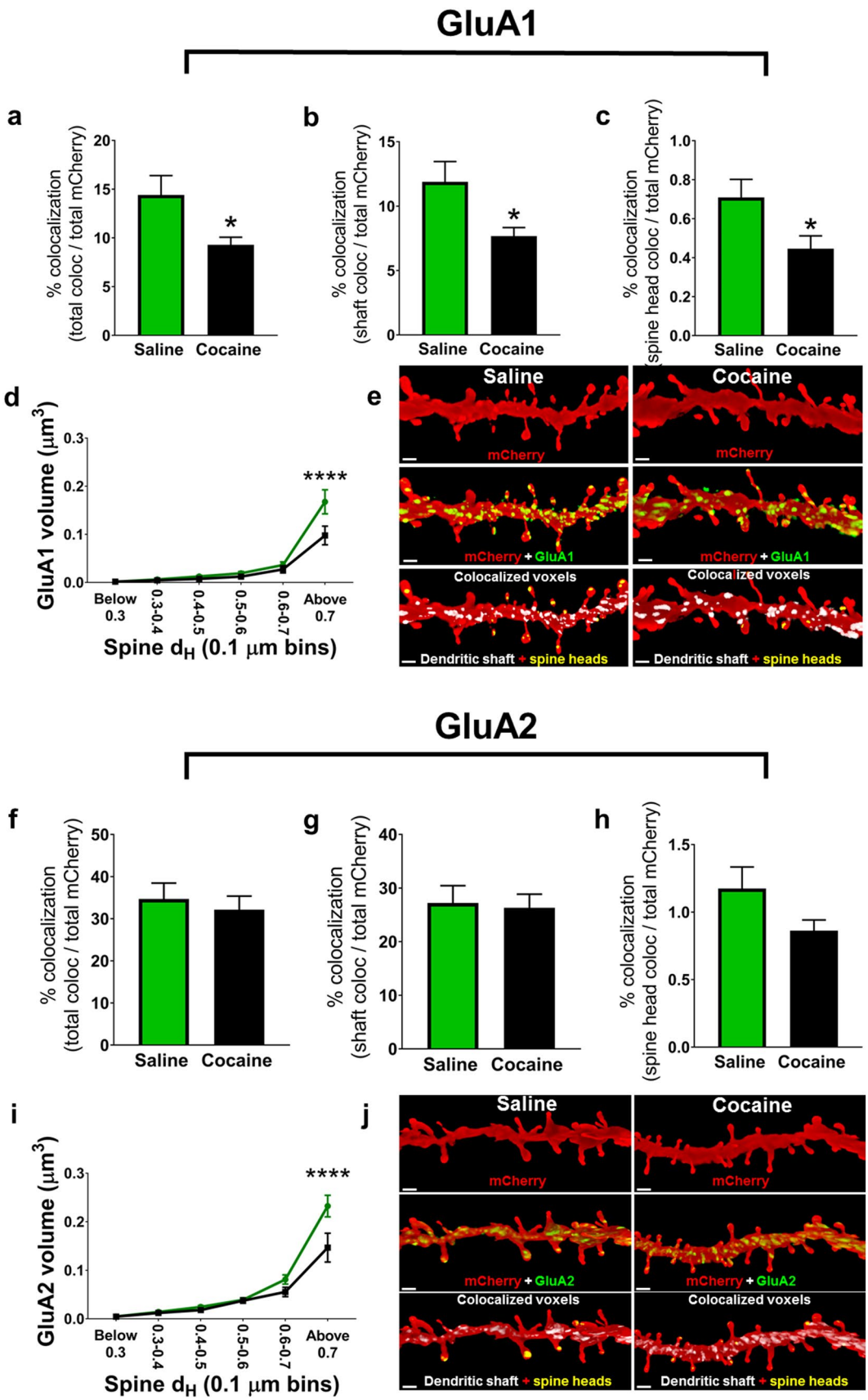
GluA1
a
% colocalization (total coloc / total mCherry)
Saline
Cocaine
b
% colocalization (shaft coloc / total mCherry)
c
% colocalization (spine head coloc / total mCherry)
d
GluA1 volume (μm³)
****
Below 0.3
0.3-0.4
0.4-0.5
0.5-0.6
0.6-0.7
Above 0.7
Spine d_H (0.1 μm bins)
e
Saline
Cocaine
mCherry
mCherry + GluA1
Colocalized voxels
Dendritic shaft + spine heads
GluA2
f
g
h
i
GluA2 volume (μm³)
j
mCherry + GluA2

◂**Fig. 3** Cocaine SA reduced GluA1/2–IR in enlarged putative mushroom spines of PrL–NA core neurons during early withdrawal. **a** Total GluA1–IR was decreased in PrL–NA core dendrites in cocaine SA rats compared to yoked-saline controls. The decreased total GluA1–IR was accounted for by **b** decreased GluA1–IR in the dendritic shaft and **c** decreased GluA1–IR in dendritic spine heads. **d** Decreased GluA1–IR in spine heads was specific to spines with d_H larger than 0.7 µm. **e** Representative dendrites from yoked-saline (left) and cocaine (right) groups showing mCherry–IR (top), mCherry$^+$/GluA1$^+$ dendrites (middle), and shaft-specific versus spine head-specific IR (bottom). **f** There was no difference between cocaine and saline in total GluA2–IR. There was no difference between cocaine and saline in dendritic shaft-specific GluA2–IR (**g**), but a trend towards decreased spine head-specific GluA2–IR (**h**) in cocaine SA rats compared to yoked-saline controls. **i** Cocaine SA rats showed decreased GluA2–IR only in spines greater than 0.7 µm. **j** Representative dendrites showing decreased spine head-specific GluA2–IR (bottom) in cocaine SA (right) compared to yoked-saline control rats (left). *p < 0.05, **$p < 0.01$, ****$p < 0.0001$ compared to saline. **a–c** Two-tailed t test. **d, i** Two-way RM ANOVA with Bonferroni-corrected pairwise comparison test. Scale bars indicate 2 µm. **a–e** $n = 6$ per group, **f–j** $n = 6$ per group

To assess the AMPA receptor expression in PrL–NA core neurons, a subset of sections was immunostained for mCherry and GluA1, as shown in Fig. S1. One yoked-saline animal showed no mCherry-labeled neurons and was not included in the analysis. We observed a significant reduction in total GluA1–IR in PrL–NA core dendrites [$t_{(10)} = 2.39$, $p = 0.04$, Fig. 3a] which was accounted for by decreased shaft-specific GluA1–IR [$t_{(10)} = 2.45$, $p = 0.03$, Fig. 3b] and spine head-specific GluA1–IR [$t_{(10)} = 2.30$, $p = 0.04$, Fig. 3c] in cocaine SA rats. Moreover, there was a significant drug by spine d_H interaction in GluA1 volume [$F_{(5,50)} = 4.18$, $p = 0.003$] and GluA1 was specifically reduced in spines with d_H larger than 0.7 µm ($p < 0.0001$, Fig. 3d) in cocaine SA rats. Representative dendritic segments are shown in Fig. 3e. Importantly, the percentage of signal above threshold did not significantly differ between groups for GluA1–IR or mCherry–IR, as shown in Fig. S4a, b, respectively, indicating that differences in GluA1–IR intensity did not contribute to the observed effect. Furthermore, we also did not observe significant differences in average GluA1–IR intensity within mCherry dendrites, as shown in Fig. S4c.

As an extension of these analyses, sections from all animals were immunostained for mCherry and GluA2. One yoked-saline animal was excluded from analysis due to immunohistochemical detection issues. The data demonstrate that total GluA2–IR was not altered during early withdrawal from cocaine SA [$t_{(10)} = 0.51$, $p = 0.62$, Fig. 3f]. There was no difference between groups in dendritic shaft-specific GluA2–IR [$t_{(10)} = 0.22$, $p = 0.83$, Fig. 3g], but there was a trend ($p = 0.11$) towards reduced spine head-specific GluA2–IR (Fig. 3h). There was a significant drug by spine d_H interaction in GluA2–IR volume [$F_{(5,50)} = 4.89$, $p = 0.001$], and GluA2–IR was specifically reduced in spines with head diameters larger than 0.7 µm ($p < 0.0001$, Fig. 3i) in cocaine SA rats. The percentage of signal above threshold was not different between groups for GluA2–IR or mCherry–IR, nor was there a difference in the average GluA2–IR intensity in mCherry$^+$ dendrites, as shown in Fig. S4d–f. Representative dendritic segments are shown in Fig. 3j.

Effect of cocaine SA on PrL–NA core spine morphometric features and PRPs after 1 week of abstinence

In Experiment 2, rats ($N = 16$) underwent 12–14 days of cocaine SA or received yoked-saline infusions. A subset of sections was used to analyze pCREB–IR in the PrL cortex. We observed no significant effect of cocaine SA on global PrL pCREB–IR during early abstinence [$t_{(4)} = 2.04$, $p = 0.11$, Fig. 4a]. When limiting analysis to PrL–NA core neurons, we observed a significant increase in the percentage of pCREB$^+$/mCherry$^+$ neurons [$t_{(4)} = 3.41$, $p = 0.02$, Fig. 4b]. Representative images are shown in Fig. 4c. There was no difference between groups in the average pCREB signal intensity in all cells that were pCREB$^+$ or in cells that were pCREB$^+$/mCherry$^+$, as shown in Fig. S2c, d, respectively.

We hypothesized that pCREB–IR in PrL–NA core neurons during early abstinence was associated with altered spine morphometric features. To address this hypothesis, we analyzed 44 dendritic segments (1907 total spines) from 6 yoked-saline rats and 48 dendritic segments (1642 total spines) from 7 cocaine SA rats. From these 13 animals, we sampled an average of 7.07 ± 1.84 (range 5–11) dendritic segments per animal. In contrast to early withdrawal, 1 week of abstinence from cocaine SA increased the average spine d_H of PrL–NA core neurons [$t_{(11)} = 7.44$, $p < 0.0001$, Fig. 4d], yet reduced spine density [$t_{(11)} = 4.32$, $p = 0.001$, Fig. 4e]. There was a significant interaction of drug and spine d_H when analyzing the percent of total spines as a function of spine d_H [$F_{(5,55)} = 18.86$, $p < 0.0001$]. Cocaine SA rats showed a reduction in the percentage of total spines with d_H between 0.3 and 0.4 µm ($p = 0.0002$) and 0.4–0.5 µm ($p = 0.003$), but an increase in the percent of total spines with head diameter above 0.7 µm ($p < 0.0001$, Fig. 4f). These changes were associated with a rightward shift in spine d_H when analyzing all spines in saline and cocaine SA rats (K–S $D = 0.19$, $p < 0.0001$, Fig. 4g). Representative dendritic segments are shown in Fig. 4h. Akin to early withdrawal, there was a positive correlation between spine d_H and pCREB–IR ($r^2 = 0.82$, $p = 0.01$, Fig. 4i), whereas there was a non-significant trend towards a negative correlation ($r^2 = 0.58$, $p = 0.07$, Fig. 4j) between spine density and pCREB–IR. There was no difference in the average spine terminal point intensity between groups, as shown in Fig. S3b.

We performed the same analyses described in Experiment 1 to quantify GluA1–IR and GluA2–IR in mCherry$^+$ dendrites. Sections from one cocaine animal did not show

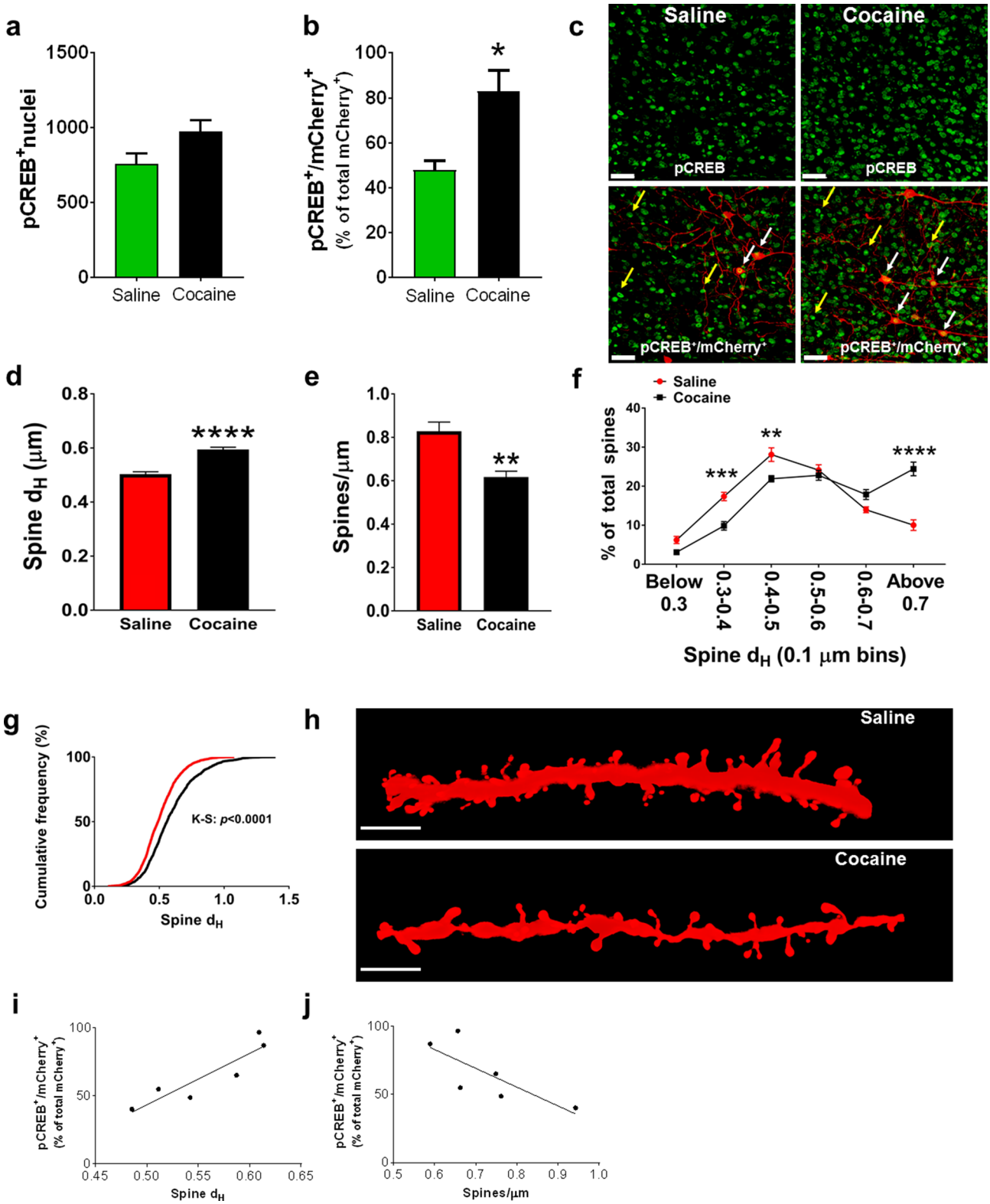

virus expression in the run processed for GluA1. There was a significant reduction in total GluA1–IR in PrL–NA core neurons [$t_{(10)} = 2.79$, $p = 0.01$, Fig. 5a] that was associated with decreased dendritic shaft-specific GluA1–IR [$t_{(10)} = 3.55$, $p = 0.005$, Fig. 5b], but increased spine head-specific GluA1–IR [$t_{(10)} = 2.50$, $p = 0.03$, Fig. 5c]. There was a significant drug by spine d_H interaction in GluA1–IR volume [$F_{(5,50)} = 11.87$, $p < 0.0001$], and GluA1–IR was specifically

◂**Fig. 4** Cocaine SA increased PrL–NA core pCREB–IR and dendritic spine head diameter during early abstinence. pCREB$^+$ neurons in layer V of the PrL cortex **(a)** and pCREB$^+$/mCherry$^+$ normalized to total mCherry$^+$ neurons **(b). c** Top-representative images of pCREB$^+$ neurons in saline and cocaine SA rats. Bottom-representative pCREB$^+$/mCherry$^+$ and pCREB$^+$/mCherry$^-$ neurons in saline and cocaine SA rats. White arrows indicate pCREB$^+$/mCherry$^+$ neurons, and yellow arrows indicate pCREB$^+$/mCherry$^-$ neurons. Cocaine SA increased PrL–NA core spine head diameter **(d)**, but decreased spine density (**e**) compared to yoked-saline controls after 1 week of abstinence. Cocaine self-administering animals show a general rightward shift in percent of total spines as a function of spine head diameter (**f**) and cumulative frequency (**g**). **h** Representative dendrites from saline and cocaine SA rats. The percentage of pCREB$^+$/mCherry$^+$ neurons positively correlated with dendritic spine head diameter (**i**) and showed a trend toward negatively correlating with dendritic spine density (**j**). *$p<0.05$, **$p<0.01$, ***$p<0.001$, ****$p<0.0001$ compared to saline. **b, d, e** Two-tailed *t* test. **f** Two-way RM ANOVA with Bonferroni-corrected pairwise comparison test. Scale bars indicate 40 µm (**e**), 5 µm (**k**). **a–c** $n=3$ per group. **d–h** $n=6$ (saline), $n=7$ (cocaine)

elevated in spines with d_H larger than 0.7 µm ($p<0.0001$, Fig. 5d) in cocaine SA rats. As above, control measurements indicate that the percentage of signal above threshold was not different between groups for GluA1–IR or mCherry–IR, nor was there a difference in average GluA1–IR intensity in mCherry$^+$ dendrites, as shown in Fig. S4g–i. Representative dendritic segments are shown in Fig. 5e.

After performing the same analyses for GluA2–IR, total GluA2–IR was unaffected after 1 week of abstinence from cocaine SA [$t_{(11)}=0.97$, $p=0.35$, Fig. 5f]. There was no difference between groups in dendritic shaft-specific GluA2–IR [$t_{(11)}=0.50$, $p=0.62$, Fig. 5g], but like GluA1, cocaine SA rats showed elevated spine head-specific GluA2–IR during early abstinence [$t_{(11)}=3.47$, $p=0.005$, Fig. 5h]. We observed a significant drug by spine d_H interaction in GluA2–IR volume [$F_{(5,55)}=5.58$, $p=0.0003$], and GluA2–IR was selectively elevated in spines with head diameters larger than 0.7 µm ($p<0.0001$, Fig. 5i). Control analyses demonstrated that the percentage of signal above threshold was not different between groups for GluA2–IR or mCherry–IR, nor was there a difference in average GluA2–IR intensity in mCherry$^+$ dendrites, as shown in Fig. S4j–l. Representative dendritic segments are shown in Fig. 5j.

Discussion

This study shows that cocaine SA produces an abstinence duration-dependent, biphasic alteration in nuclear and dendritic spine PRPs and dendritic spine morphology of PrL–NA core neurons. During early withdrawal, nuclear Fos–IR, pCREB–IR, as well as spine d_H in PrL–NA core neurons were decreased, whereas total GluA1–IR, but not total GluA2–IR, was diminished in PrL–NA core dendrites. However, both AMPA receptor subunits were reduced in putative mushroom-type spines. In contrast, after 1 week of abstinence, pCREB–IR in the nucleus of PrL–NA core neurons and spine d_H was elevated, but dendritic spines were decreased in quantity in PrL–NA core neurons. As in early withdrawal, total GluA1–IR, but not GluA2–IR, was reduced in PrL–NA core neurons, but both AMPA receptor subunits were elevated in dendritic spine heads of PrL–NA core neurons, an effect associated with an increase in putative mushroom-type spines. Figure 6 summarizes these adaptations at both abstinence timepoints.

Cocaine SA reduced nuclear activity markers, dendritic spine d_H, and GluA1/2 spine head localization in PrL–NA core neurons during early withdrawal

Although there was no significant effect of early withdrawal from cocaine SA on global Fos–IR or pCREB–IR in the nucleus of PrL–NA core neurons during early withdrawal from cocaine SA, there was a significant decrease in Fos–IR and pCREB–IR selectively in the nucleus of PrL–NA core neurons. This evidence extends the previous data from our laboratory, showing that cocaine SA leads to a decrease in phospho-protein signaling in the PrL cortex during early withdrawal (Sun et al. 2013; Whitfield et al. 2011; Go et al. 2016; Barry and McGinty 2017) and extends the findings specifically to PrL–NA core neurons.

Alterations in Fos and CREB expressions are linked to changes in dendritic spine morphological properties (Middei et al. 2013, 2012; Pignataro et al. 2015; Matsuzaki et al. 2001). Albeit correlative, we found that animals which had lower spine d_H (i.e., cocaine SA animals) tended to have lower nuclear pCREB–IR in PrL–NA core neurons, suggesting a link between CREB-mediated gene transcriptional activity in the nucleus of PrL–NA core neurons and apical tuft spine morphology. This finding is consistent with findings, showing that the expression of a dominant negative phospho-deficient mutation of pCREB^{S133} prevents dendritic spine formation associated with contextual fear learning (Middei et al. 2012) and decreasing the likelihood that neurons expressing mutated CREB are represented in a neuronal ensemble encoding a fear memory context (Han et al. 2007). Moreover, this mutation decreases basal and learning-induced GluA1 synaptic incorporation that is associated with a decrease in long-term potentiation and an increase in long-term depression in the hippocampus (Middei et al. 2013). GluA1 and pCREB are linked functionally as well as transcriptionally, since the promoter region of *Gria1* contains four cyclase response elements that bind pCREB and regulate *Gria1* gene expression (Borges and Dingledine 2001). Thus, decreased pCREB–IR and spine d_H are likely linked to decreased AMPA expression

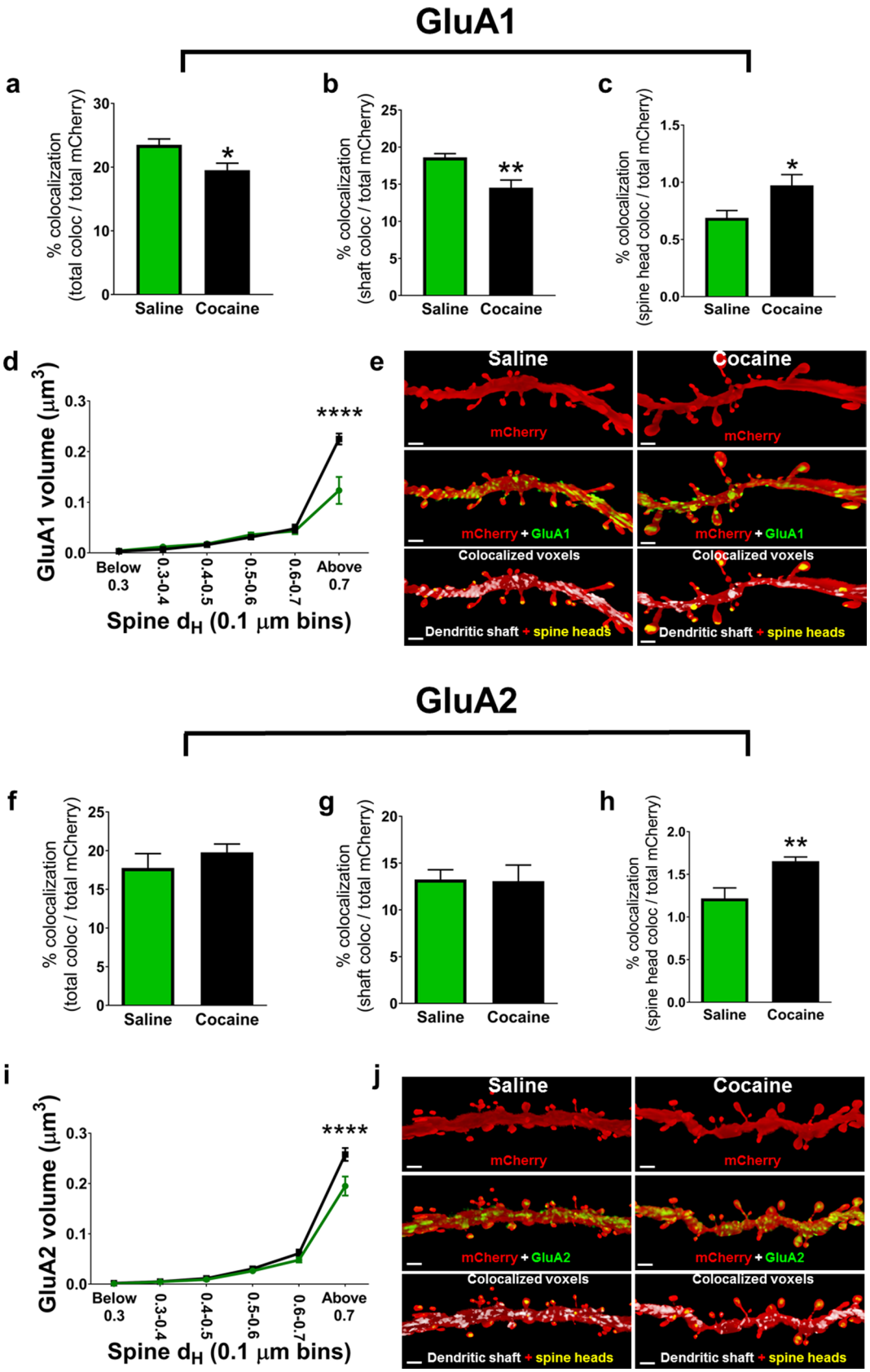
GluA1
a
% colocalization (total coloc / total mCherry)
Saline
Cocaine
b
% colocalization (shaft coloc / total mCherry)
c
% colocalization (spine head coloc / total mCherry)
d
GluA1 volume (μm³)
Below 0.3
0.3-0.4
0.4-0.5
0.5-0.6
0.6-0.7
Above 0.7
Spine d_H (0.1 μm bins)
e
Saline
Cocaine
mCherry
mCherry + GluA1
Colocalized voxels
Dendritic shaft + spine heads
GluA2
f
g
h
i
GluA2 volume (μm³)
j
mCherry + GluA2

◂**Fig. 5** Cocaine SA increased GluA1/2–IR in enlarged mushroom spines of PrL–NA core neurons during early abstinence. **a** Total GluA1–IR was decreased in PrL–NA core dendrites. This was accounted for by **b** decreased GluA1–IR in the dendritic shaft, but **(c)** increased GluA1–IR in dendritic spine heads. **d** Increased GluA1–IR in spine heads was specific to spines with head diameters larger than 0.7 µm compared to yoked-saline controls. **e** Representative dendrites from saline (left) and cocaine (right) showing mCherry (top), $mCherry^{+}/GluA1^{+}$ dendrites (middle), and dendritic shaft-specific versus spine head-specific GluA1–IR (bottom). **f** There was no difference between cocaine and yoked-saline in total GluA2–IR. There was no difference between cocaine and saline in shaft-specific GluA2–IR (**g**), but a significant increase in spine head-specific GluA2–IR (**h**). **i** Cocaine SA rats showed increased GluA2–IR only in spine heads greater than 0.7 µm compared to yoked-saline controls. **j** Representative dendrites from saline (left) and cocaine (right) showing mCherry (top), $mCherry^{+}$ $GluA2^{+}$ dendrites (middle), and dendritic shaft-specific versus spine head-specific GluA2–IR (bottom). $^{*}p<0.05$, $^{**}p<0.01$, $^{****}p<0.0001$ compared to saline. **a–c, h** Two-tailed *t* test. **d, i** Two-way RM ANOVA with Bonferroni-corrected pairwise comparison test. Scale bars 2 µm. **a–e** $n=6$ per group, **f–j**: $n=6$ (saline), $n=7$ (cocaine)

in PrL–NA core dendrites and spines, translating into long-term depression.

There were distinct yet overlapping alterations in AMPA receptor subunit expression in PrL–NA core dendrites and spines. Whereas GluA1–IR was globally suppressed in PrL–NA core neurons, GluA2–IR was only reduced in a specific subset of dendritic spines (i.e., enlarged, mushroom-type spines). There are precedents for differential regulation of AMPA receptor expression; these two subunits undergo differential trafficking in dendrites and spines due to heterogenous interactions with subunit-specific AMPA receptor-interacting proteins (Shepherd and Huganir 2007; Anggono and Huganir 2012). Furthermore, GluA1 and GluA2 differentially regulate spine morphology (Prithviraj et al. 2008), with GluA2 playing a key role in spine morphogenesis in vitro by interacting with the cell-adhesion molecule N-cadherin (Passafaro et al. 2003; Saglietti et al. 2007). Although our findings indicate that early withdrawal differentially regulates total GluA1–IR and GluA2–IR in PrL–NA core neurons, our data demonstrating that both subunits were reduced in enlarged dendritic spines, in which the majority of AMPA receptor expression and function occurs (Matsuzaki et al. 2001), indicate that mature spines undergo AMPA receptor removal during early withdrawal from cocaine. Future studies will examine the molecular mechanisms underlying the cocaine-induced dendritic spine morphological adaptations and associated GluA1 and GluA2 mobilization.

1 week of abstinence from cocaine SA increased pCREB expression in PrL–NA core neurons and increased GluA1/2 IR in dendritic spines with large spine heads

In a previous study, in contrast to early withdrawal, after 1 week of abstinence from cocaine SA, PKA-mediated hyper-phosphorylation of $CREB^{S133}$ and $GluA1^{S845}$ in the PrL cortex develops (Sun et al. 2014a). Stimulation of the PKA-GluA1 pathway by catecholamines lowers the threshold for LTP induction (Hu et al. 2007), indicating that PKA-mediated $GluA1^{S845}$ phosphorylation primes AMPA receptors for synaptic incorporation, as shown previously with D1-PKA-GluA1 in cultured prefrontal cortical neurons (Sun et al. 2005). Inhibiting PKA activity at this abstinence timepoint with an intra-PrL microinfusion of Rp-cAMPs suppressed context-induced cocaine seeking (Sun et al. 2014a), linking PKA-mediated $pCREB^{S133}$ and $GluA1^{S845}$ phosphorylation to relapse. Here, we extend our previous findings by demonstrating that elevated $pCREB^{S133}$ and GluA1–IR are observed in PrL–NA core nuclei and spines, respectively.

One interpretation of these data is that the augmentation of PRPs and spine d_H render PrL–NA core neurons hyper-excitable to glutamate inputs during early abstinence, increasing the likelihood that these neurons are selectively involved in the memory trace encoding the salience of the cocaine-conditioned context. This interpretation is supported by findings, showing that the overexpression of CREB in a subset of amygdala neurons increases the likelihood that these neurons are involved in a neuronal ensemble encoding a fear memory context (Han et al. 2007), perhaps through CREB-mediated increases in intrinsic excitability (Yiu et al. 2014; Han et al. 2007) or stabilization of individual excitatory synapses (Lisman et al. 2018). The increase in nuclear pCREB and the potential for subsequent increased excitability following abstinence from cocaine SA are supported by recent data, indicating that extinction from cocaine SA increases the intrinsic excitability of layer V PrL neurons, an effect required for cue-induced reinstatement (Sepulveda-Orengo et al. 2017; Parrilla-Carrero et al. 2018). Similarly, cocaine-conditioned place preference (CPP) training increases evoked AMPA receptor-mediated excitatory transmission in layer V PrL cortical neurons and normalization of this adaptation prevents subsequent CPP memory retrieval (Otis and Mueller 2017). As discussed above, stabilization of individual excitatory synapses may be one function of enhanced pCREB in PrL–NA core neurons, which is associated with changes in morphological properties of dendritic spines and associated AMPA receptor expression (Kasai et al. 2003; Tanaka et al. 2008; Matsuzaki et al. 2004).

In contrast to early withdrawal, cocaine SA followed by early (1 week) or more prolonged (2 weeks to 1 month) abstinence has previously been shown to alter structural

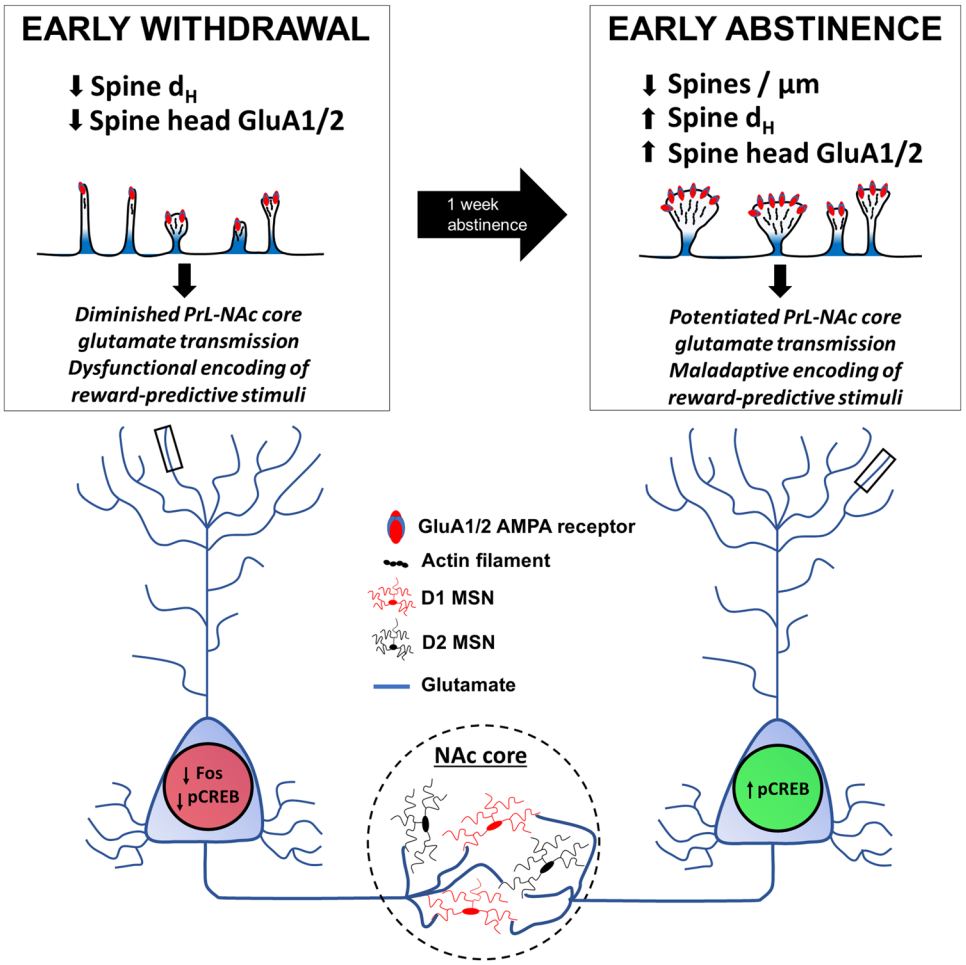

Fig. 6 Diagram showing abstinence duration-dependent biphasic alterations in spine morphology and plasticity-related proteins in PrL–NA core neurons. During early withdrawal from cocaine SA, decreased spine d_H, nuclear Fos–iR and pCREB–IR, and GluA1/2–IR in mature dendritic spines occurs. However, after 1 week of abstinence, spine d_H, pCREB, and GluA1/2 expression in mature dendritic spines are increased. This chain of events likely leads to dysfunctional encoding of cocaine-predictive stimuli, ultimately driving relapse following reintroduction of cocaine-paired contexts

plasticity within the PrL cortex (Radley et al. 2015; Robinson et al. 2001; Rasakham et al. 2014). However, conflicting reports have emerged regarding the nature and extent of abstinence-induced PrL structural plasticity. Our data indicate that cocaine SA followed by 1 week of abstinence decreased the density of PrL–NA core neuron apical dendritic spines, yet increased the spine d_H. The extant literature on layer V PrL cortical structural plasticity at this timepoint reports increased layer V basal thin spine density, but decreased synapse number and overall dendritic complexity (Rasakham et al. 2014). Our results are complementary to this finding, because our data derive from pathway-specific structural modifications. Moreover, the region of dendrite investigated is also an important factor, as inputs to the apical tuft (Liu and Aghajanian 2008) and basal dendrites (Liu et al. 2015) differ in their origin. Finally, our findings are in general agreement with recent experiments utilizing similar methodology demonstrating decreased apical spine density of PrL neurons specifically projecting to D1-expressing MSNs in the NA core following 2 weeks of abstinence from a sensitizing regimen of cocaine administration (Barrientos et al. 2018).

Regarding AMPA receptor plasticity during early abstinence, in contrast to early withdrawal, we found decreased dendritic shaft-specific, but elevated spine head-specific, GluA1–IR, and increased spine head-specific GluA2–IR. These findings demonstrate dendritic compartment-specific changes in GluA1–IR in PrL–NA core neurons after 1 week of abstinence that are distinct from those that occur during early withdrawal. Although it has been well-characterized that GluA2-lacking AMPA receptors in the NA core play a central role in incubation of cocaine seeking after prolonged abstinence in long-access SA paradigms (Conrad et al. 2008), we did not detect GluA2-lacking AMPA receptors in the PrL cortex in our model, since both AMPA receptor subunits were increased in dendritic spines of PrL–NA core neurons after 1 week of abstinence. However, we cannot exclude effects on GluA3/4-containing AMPA receptors after cocaine SA. Regardless, increased AMPA receptor expression in enlarged dendritic spines likely disposes these dendritic compartments to be hypersensitive to glutamate release, given that spines with enlarged volume show greater AMPA receptor-mediated currents (Matsuzaki et al. 2001, 2004). Moreover,

because we found an overall decrease in spine density, but increased spine d_H associated with increased AMPA–IR in enlarged spines, it is intriguing to hypothesize that specific inputs to the distal apical tuft of PrL–NA core neurons may be potentiated, whereas others are depressed. This is supported by the previous work, showing that spines adjacent to active synapses have an accumulation of AMPA receptors leading to a lack of lateral diffusion (i.e., functional trapping at synapses), but AMPA receptors within spines adjacent to inactive synapses rapidly diffuse away from synaptic sites (Ehlers et al. 2007).

Potential inputs to PrL–NA core neurons and functional implications

Layer V prefrontal cortical pyramidal neurons receive dense glutamatergic inputs arising from cortico-cortical and thalamocortical neurons (Berendse and Groenewegen 1991). The axon boutons of thalamocortical neurons are under the control of several neuromodulators, including orexin, acetylcholine, and serotonin. Accordingly, orexin application to mPFC slices elicits thalamocortical glutamate release onto apical dendritic spines of layer V PrL neurons, driving postsynaptic Ca^{2+} transients in only a subset of those spines (Lambe and Aghajanian 2003). Moreover, stimulation of α4β2 nicotinic acetylcholine receptors also induces glutamate release onto layer V PrL cortical pyramidal neurons due to actions at axon boutons of thalamocortical neurons (Lambe et al. 2003). Finally, serotonin application to apical, but not basal, layer V PrL cortical dendrites elicits EPSCs in layer V PrL cortical neurons (Aghajanian and Marek 1997), an effect eliminated by chronic stress, which leads to apical dendrite atrophy (Liu and Aghajanian 2008). Given the link between chronic stress-induced dendritic atrophy and cocaine SA-induced spine morphometric adaptations in the PrL cortex (Radley et al. 2015), it is possible that the alterations in PrL–NA core spine morphometric features and PRPs observed during early withdrawal are due to alterations in thalamocortical glutamate release and its regulation by the aforementioned neuromodulators. One possible scenario is that daily cocaine SA sessions lead to time-dependent increases in glutamate release onto layer V PrL–NA core apical dendritic spines arising from thalamocortical neurons, promoting encoding of cocaine-associated sensory stimuli. However, PrL–NA core neurons may compensate for augmented glutamate release by reducing the size of dendritic spines and AMPA receptor occupancy in apical spine heads, leading to reduced phospho-protein signaling, during early withdrawal from cocaine SA. The identity and functional role of the salient inputs that are responsible for the observed effects of cocaine SA at both abstinence timepoints will be a focus of future investigation.

Time-dependent role of BDNF and PKA in regulating PrL–NA core PRPs

Our previous studies demonstrate that intra-PrL administration of BDNF reverses cocaine's impact on phospho-protein signaling during early withdrawal, thereby reducing drug seeking (Berglind et al. 2007; Go et al. 2016). The data reported herein are consistent with the global changes in PrL cortex that we have previously reported and suggest that the changes in PRPs and dendritic spines in the PrL–NA core pathway during early withdrawal also contribute to relapse and would be reversed by intra-PrL BDNF. Glutamate uncaging at single spines of CA1 pyramidal neurons rapidly increases dendritic spine head size, which is dependent on BDNF–TrkB signaling, and exogenous BDNF application combined with glutamate uncaging produces a more sustained increase in spine head size relative to glutamate uncaging alone (Tanaka et al. 2008). Thus, it is likely that a single BDNF microinfusion increases AMPA receptor accumulation in dendritic spines which likely requires sustained spine head enlargement. However, other relevant downstream pathways related to the regulation of actin polymerization by BDNF–TrkB signaling are likely also involved. Ultimately, these effects may lead to a normalization of glutamate transmission in the PrL–NA core pathway. This hypothesis is supported by the previous data, indicating that a single BDNF microinfusion in the PrL cortex immediately after the final SA session leads to a long-term normalization of extracellular glutamate in the NA core and prevents cocaine prime-induced elevations in extracellular glutamate (Berglind et al. 2009).

In contrast, over the course of 1 week of abstinence, PrL–NA core neurons appear to undergo allostatic alterations in structure and function to counteract the early withdrawal effects of cocaine on PRPs, leading to enhanced encoding of cocaine-conditioned stimuli that takes time to develop. These effects would be impervious to BDNF application after 1 week of abstinence, because intra-PrL BDNF is unable to suppress relapse when microinfused after 1 week of abstinence (Berglind et al. 2007). Moreover, ERK phosphorylation is normal 24 h and 7 days after the final cocaine SA session (Whitfield et al. 2011). Instead, adaptations in PrL–NA core structural plasticity and PRPs after 1 week of abstinence would likely be responsive to PKA inhibition, as our previous data derived from western blotting show (Sun et al. 2014a). Thus, the transition from hypotrophic spine morphology and decreased nuclear pCREB to hypertrophic spine morphology and increased nuclear pCREB in PrL–NA core neurons likely develops as a result of a switch from ERK-dependent to PKA-dependent regulation as a function of abstinence duration. In future studies, we will examine additional timepoints during abstinence and the effects of BDNF and PKA inhibition on associated

structural and synaptic plasticity. The functional relevance of these changes in PrL–NA core neurons to drug seeking is also the subject of further investigation.

Conclusions

Our findings link previously described biphasic alterations in glutamatergic signaling occurring globally in the PrL cortex during early withdrawal and early abstinence with similar adaptations in the PrL–NA core pathway. These adaptations occur not only in the nucleus of PrL–NA core neurons, but also at the level of individual dendritic spines, leading to differential compartmentalization of AMPA receptors in spines and dendritic shafts at different times after cocaine exposure. Given that there is remarkable dichotomy in PrL–NA core adaptations at the two timepoints studied, we hypothesize that the altered structure and, presumably diminished function, of PrL–NA core neurons during early withdrawal likely trigger the subsequent enlargement of dendritic spines, induction of pCREB, and accumulation of AMPA receptors in enlarged spines in these neurons after 1 week of abstinence (Fig. 6). Thus, the abstinence duration-dependent adaptations in PrL–NA core neurons provide a novel way of interpreting PrL–NA core dysfunction pertaining to relapse vulnerability. Moreover, these findings suggest that treatments for relapse vulnerability in clinical populations should consider the timing at which interventions occur given the heterogeneity in PRP adaptations in critical brain regions over the course of abstinence.

Acknowledgements We thank Jordan Hopkins and Kaylee Hooker for excellent technical assistance. This work was supported by National Institute on Drug Abuse Grants: P50 DA15369 (JFM), R01 DA033479 (JFM), T32 DA007288 (JFM), F31 DA041021 (BMS), and R00 DA040004 (MDS).

Compliance with ethical standards

Conflict of interest The authors declare that they have no conflict of interest.

Ethical standards All procedures performed in studies involving animals were in accordance with the ethical standards of the institution or practice at which the studies were conducted. This article does not contain any studies with human participants performed by any of the authors.

References

Aghajanian GK, Marek GJ (1997) Serotonin induces excitatory postsynaptic potentials in apical dendrites of neocortical pyramidal cells. Neuropharmacology 36:589–599

Anggono V, Huganir RL (2012) Regulation of AMPA receptor trafficking and synaptic plasticity. Curr Opin Neurobiol 22:461–469. https://doi.org/10.1016/j.conb.2011.12.006

Ball KT, Wellman CL, Fortenberry E, Rebec GV (2009) Sensitizing regimens of (±)3, 4-methylenedioxymethamphetamine (ecstasy) elicit enduring and differential structural alterations in the brain motive circuit of the rat. Neuroscience 160:264–274. https://doi.org/10.1016/j.neuroscience.2009.02.025

Banke TG, Bowie D, Lee H, Huganir RL, Schousboe A, Traynelis SF (2000) Control of GluR1 AMPA receptor function by cAMP-dependent protein kinase. J Neurosci 20:89–102

Barrientos C, Knowland D, Wu MMJ, Lilascharoen V, Huang KW, Malenka RC, Lim BK (2018) Cocaine induced structural plasticity in input regions to distinct cell types in nucleus accumbens. Biol Psychiatry. https://doi.org/10.1016/j.biopsych.2018.04.019

Barry SM, McGinty JF (2017) Role of Src family kinases in BDNF-mediated suppression of cocaine-seeking and prevention of cocaine-induced ERK, GluN2A, and GluN2B dephosphorylation in the prelimbic cortex. Neuropsychopharmacology 42:1972–1980. https://doi.org/10.1038/npp.2017.114

Berendse HW, Groenewegen HJ (1991) Restricted cortical termination fields of the midline and intralaminar thalamic nuclei in the rat. Neuroscience 42:73–102

Berglind WJ, Whitfield TW Jr, LaLumiere RT, Kalivas PW, McGinty JF (2009) A single intra-PFC infusion of BDNF prevents cocaine-induced alterations in extracellular glutamate within the nucleus accumbens. J Neurosci 29:3715–3719. https://doi.org/10.1523/JNEUROSCI.5457-08.2009

Berglind WJ, See RE, Fuchs RA, Ghee SM, Whitfield TW Jr, Miller SW, McGinty JF (2007) A BDNF infusion into the medial prefrontal cortex suppresses cocaine seeking in rats. Eur J Neurosci 26:757–766. https://doi.org/10.1111/j.1460-9568.2007.05692.x

Borges K, Dingledine R (2001) Functional organization of the GluR1 glutamate receptor promoter. J Biol Chem 276:25929–25938. https://doi.org/10.1074/jbc.M009105200

Chen BT, Yau HJ, Hatch C, Kusumoto-Yoshida I, Cho SL, Hopf FW, Bonci A (2013) Rescuing cocaine-induced prefrontal cortex hypoactivity prevents compulsive cocaine seeking. Nature 496:359–362. https://doi.org/10.1038/nature12024

Conrad KL, Tseng KY, Uejima JL, Reimers JM, Heng LJ, Shaham Y, Marinelli M, Wolf ME (2008) Formation of accumbens GluR2-lacking AMPA receptors mediates incubation of cocaine craving. Nature 454:118–121. https://doi.org/10.1038/nature06995

Dennis TS, Jhou TC, McGinty JF (2018) Cocaine self-administration and time-dependent decreases in prelimbic activity. bioRxiv. https://doi.org/10.1101/255455

Dos Santos M, Salery M, Forget B, Garcia Perez MA, Betuing S, Boudier T, Vanhoutte P, Caboche J, Heck N (2017) Rapid Synaptogenesis in the nucleus accumbens is induced by a single cocaine administration and stabilized by mitogen-activated protein kinase interacting kinase-1 activity. Biol Psychiatry 82:806–818. https://doi.org/10.1016/j.biopsych.2017.03.014

Ehlers MD, Heine M, Groc L, Lee MC, Choquet D (2007) Diffusional trapping of GluR1 AMPA receptors by input-specific synaptic activity. Neuron 54:447–460. https://doi.org/10.1016/j.neuron.2007.04.010

Giannotti G, Barry SM, Siemsen BM, Peters J, McGinty JF (2018) Divergent prelimbic cortical pathways control BDNF-dependent vs. independent suppression of cocaine seeking. J Neurosci 38:8956–8966

Gipson CD, Kupchik YM, Shen H, Reissner KJ, Thomas CA, Kalivas PW (2013) Relapse induced by cues predicting cocaine depends on rapid, transient synaptic potentiation. Neuron 77:867–872. https://doi.org/10.1016/j.neuron.2013.01.005

Go BS, Barry SM, McGinty JF (2016) Glutamatergic neurotransmission in the prefrontal cortex mediates the suppressive effect

of intra-prelimbic cortical infusion of BDNF on cocaine-seeking. Eur Neuropsychopharmacol 26:1989–1999. https://doi.org/10.1016/j.euroneuro.2016.10.002

Han JH, Kushner SA, Yiu AP, Cole CJ, Matynia A, Brown RA, Neve RL, Guzowski JF, Silva AJ, Josselyn SA (2007) Neuronal competition and selection during memory formation. Science 316:457–460. https://doi.org/10.1126/science.1139438

Hu H, Real E, Takamiya K, Kang MG, Ledoux J, Huganir RL, Malinow R (2007) Emotion enhances learning via norepinephrine regulation of AMPA-receptor trafficking. Cell 131:160–173. https://doi.org/10.1016/j.cell.2007.09.017

Kalivas PW (2009) The glutamate homeostasis hypothesis of addiction. Nat Rev Neurosci 10:561–572. https://doi.org/10.1038/nrn2515

Kalivas PW, Volkow N, Seamans J (2005) Unmanageable motivation in addiction: a pathology in prefrontal-accumbens glutamate transmission. Neuron 45:647–650. https://doi.org/10.1016/j.neuron.2005.02.005

Kasai H, Matsuzaki M, Noguchi J, Yasumatsu N, Nakahara H (2003) Structure-stability-function relationships of dendritic spines. Trends Neurosci 26:360–368. https://doi.org/10.1016/S0166-2236(03)00162-0

Lambe EK, Aghajanian GK (2003) Hypocretin (orexin) induces calcium transients in single spines postsynaptic to identified thalamocortical boutons in prefrontal slice. Neuron 40:139–150

Lambe EK, Picciotto MR, Aghajanian GK (2003) Nicotine induces glutamate release from thalamocortical terminals in prefrontal cortex. Neuropsychopharmacology 28:216–225. https://doi.org/10.1038/sj.npp.1300032

Larkum ME, Nevian T, Sandler M, Polsky A, Schiller J (2009) Synaptic integration in tuft dendrites of layer 5 pyramidal neurons: a new unifying principle. Science 325:756–760. https://doi.org/10.1126/science.1171958

Lisman J, Cooper K, Sehgal M, Silva AJ (2018) Memory formation depends on both synapse-specific modifications of synaptic strength and cell-specific increases in excitability. Nat Neurosci 21:309–314. https://doi.org/10.1038/s41593-018-0076-6

Liu RJ, Aghajanian GK (2008) Stress blunts serotonin- and hypocretin-evoked EPSCs in prefrontal cortex: role of corticosterone-mediated apical dendritic atrophy. Proc Natl Acad Sci USA 105:359–364. https://doi.org/10.1073/pnas.0706679105

Liu RJ, Ota KT, Dutheil S, Duman RS, Aghajanian GK (2015) Ketamine strengthens CRF-activated amygdala inputs to basal dendrites in mPFC layer V pyramidal cells in the prelimbic but not infralimbic subregion, a key suppressor of stress responses. Neuropsychopharmacology 40:2066–2075. https://doi.org/10.1038/npp.2015.70

Matsuo N, Reijmers L, Mayford M (2008) Spine-type-specific recruitment of newly synthesized AMPA receptors with learning. Science 319:1104–1107. https://doi.org/10.1126/science.1149967

Matsuzaki M, Ellis-Davies GC, Nemoto T, Miyashita Y, Iino M, Kasai H (2001) Dendritic spine geometry is critical for AMPA receptor expression in hippocampal CA1 pyramidal neurons. Nat Neurosci 4:1086–1092. https://doi.org/10.1038/nn736

Matsuzaki M, Honkura N, Ellis-Davies GC, Kasai H (2004) Structural basis of long-term potentiation in single dendritic spines. Nature 429:761–766. https://doi.org/10.1038/nature02617

Middei S, Spalloni A, Longone P, Pittenger C, O'Mara SM, Marie H, Ammassari-Teule M (2012) CREB selectively controls learning-induced structural remodeling of neurons. Learn Mem 19:330–336. https://doi.org/10.1101/lm.025817.112

Middei S, Houeland G, Cavallucci V, Ammassari-Teule M, D'Amelio M, Marie H (2013) CREB is necessary for synaptic maintenance and learning-induced changes of the AMPA receptor GluA1 subunit. Hippocampus 23:488–499. https://doi.org/10.1002/hipo.22108

Otis JM, Mueller D (2017) Reversal of cocaine-associated synaptic plasticity in medial prefrontal cortex parallels elimination of memory retrieval. Neuropsychopharmacology 42:2000–2010. https://doi.org/10.1038/npp.2017.90

Otis JM, Namboodiri VM, Matan AM, Voets ES, Mohorn EP, Kosyk O, McHenry JA, Robinson JE, Resendez SL, Rossi MA, Stuber GD (2017) Prefrontal cortex output circuits guide reward seeking through divergent cue encoding. Nature 543:103–107. https://doi.org/10.1038/nature21376

Parrilla-Carrero J, Buchta WC, Goswamee P, Culver O, McKendrick G, Harlan B, Moutal A, Penrod R, Lauer A, Ramakrishnan V, Khanna R, Kalivas P, Riegel AC (2018) Restoration of Kv7 channel-mediated inhibition reduces cued-reinstatement of cocaine seeking. J Neurosci 38:4212–4229. https://doi.org/10.1523/JNEUROSCI.2767-17.2018

Passafaro M, Nakagawa T, Sala C, Sheng M (2003) Induction of dendritic spines by an extracellular domain of AMPA receptor subunit GluR2. Nature 424:677–681. https://doi.org/10.1038/nature01781

Pignataro A, Borreca A, Ammassari-Teule M, Middei S (2015) CREB regulates experience-dependent spine formation and enlargement in mouse barrel cortex. Neural Plast 2015:651469. https://doi.org/10.1155/2015/651469

Prithviraj R, Kelly KM, Espinoza-Lewis R, Hexom T, Clark AB, Inglis FM (2008) Differential regulation of dendrite complexity by AMPA receptor subunits GluR1 and GluR2 in motor neurons. Dev Neurobiol 68:247–264. https://doi.org/10.1002/dneu.20590

Radley JJ, Anderson RM, Cosme CV, Glanz RM, Miller MC, Romig-Martin SA, LaLumiere RT (2015) The contingency of cocaine administration accounts for structural and functional medial prefrontal deficits and increased adrenocortical activation. J Neurosci 35:11897–11910. https://doi.org/10.1523/JNEUROSCI.4961-14.2015

Rasakham K, Schmidt HD, Kay K, Huizenga MN, Calcagno N, Pierce RC, Spires-Jones TL, Sadri-Vakili G (2014) Synapse density and dendritic complexity are reduced in the prefrontal cortex following seven days of forced abstinence from cocaine self-administration. PLoS One 9:e102524. https://doi.org/10.1371/journal.pone.0102524

Robinson TE, Gorny G, Mitton E, Kolb B (2001) Cocaine self-administration alters the morphology of dendrites and dendritic spines in the nucleus accumbens and neocortex. Synapse 39:257–266. https://doi.org/10.1002/1098-2396(20010301)39:3%3C257::AID-SYN1007%3E3.0.CO;2-1

Russo SJ, Dietz DM, Dumitriu D, Morrison JH, Malenka RC, Nestler EJ (2010) The addicted synapse: mechanisms of synaptic and structural plasticity in nucleus accumbens. Trends Neurosci 33:267–276. https://doi.org/10.1016/j.tins.2010.02.002

Saglietti L, Dequidt C, Kamieniarz K, Rousset MC, Valnegri P, Thoumine O, Beretta F, Fagni L, Choquet D, Sala C, Sheng M, Passafaro M (2007) Extracellular interactions between GluR2 and N-cadherin in spine regulation. Neuron 54:461–477. https://doi.org/10.1016/j.neuron.2007.04.012

Scofield MD, Li H, Siemsen BM, Healey KL, Tran PK, Woronoff N, Boger HA, Kalivas PW, Reissner KJ (2016) Cocaine self-administration and extinction leads to reduced glial fibrillary acidic protein expression and morphometric features of astrocytes in the nucleus accumbens core. Biol Psychiatry 80:207–215. https://doi.org/10.1016/j.biopsych.2015.12.022

Sepulveda-Orengo MT, Healey KL, Kim R, Auriemma AC, Rojas J, Woronoff N, Hyppolite R, Reissner KJ (2017) Riluzole impairs cocaine reinstatement and restores adaptations in intrinsic excitability and GLT-1 expression. Neuropsychopharmacology. https://doi.org/10.1038/npp.2017.244

Shepherd JD, Huganir RL (2007) The cell biology of synaptic plasticity: AMPA receptor trafficking. Annu Rev Cell Dev Biol 23:613–643. https://doi.org/10.1146/annurev.cellbio.23.090506.123516

Siemsen BM, Lombroso PJ, McGinty JF (2018) Intra-prelimbic cortical inhibition of striatal-enriched tyrosine phosphatase suppresses cocaine seeking in rats. Addict Biol 23:219–229. https://doi.org/10.1111/adb.12504

Spencer S, Garcia-Keller C, Roberts-Wolfe D, Heinsbroek JA, Mulvaney M, Sorrell A, Kalivas PW (2017) Cocaine use reverses striatal plasticity produced during cocaine seeking. Biol Psychiatry 81:616–624. https://doi.org/10.1016/j.biopsych.2016.08.033

Stefanik MT, Kupchik YM, Kalivas PW (2016) Optogenetic inhibition of cortical afferents in the nucleus accumbens simultaneously prevents cue-induced transient synaptic potentiation and cocaine-seeking behavior. Brain Struct Funct 221:1681–1689. https://doi.org/10.1007/s00429-015-0997-8

Sun X, Zhao Y, Wolf ME (2005) Dopamine receptor stimulation modulates AMPA receptor synaptic insertion in prefrontal cortex neurons. J Neurosci 25:7342–7351. https://doi.org/10.1523/JNEUROSCI.4603-04.2005

Sun WL, Zelek-Molik A, McGinty JF (2013) Short and long access to cocaine self-administration activates tyrosine phosphatase STEP and attenuates GluN expression but differentially regulates GluA expression in the prefrontal cortex. Psychopharmacology 229:603–613. https://doi.org/10.1007/s00213-013-3118-5

Sun WL, Coleman NT, Zelek-Molik A, Barry SM, Whitfield TW Jr, McGinty JF (2014a) Relapse to cocaine-seeking after abstinence is regulated by cAMP-dependent protein kinase A in the prefrontal cortex. Addict Biol 19:77–86. https://doi.org/10.1111/adb.12043

Sun WL, Eisenstein SA, Zelek-Molik A, McGinty JF (2014b) A single brain-derived neurotrophic factor infusion into the dorsomedial prefrontal cortex attenuates cocaine self-administration-induced phosphorylation of synapsin in the nucleus accumbens during early withdrawal. Int J Neuropsychopharmacol. https://doi.org/10.1093/ijnp/pyu049

Szepesi Z, Hosy E, Ruszczycki B, Bijata M, Pyskaty M, Bikbaev A, Heine M, Choquet D, Kaczmarek L, Wlodarczyk J (2014) Synaptically released matrix metalloproteinase activity in control of structural plasticity and the cell surface distribution of GluA1-AMPA receptors. PLoS One 9:e98274. https://doi.org/10.1371/journal.pone.0098274

Tanaka J, Horiike Y, Matsuzaki M, Miyazaki T, Ellis-Davies GC, Kasai H (2008) Protein synthesis and neurotrophin-dependent structural plasticity of single dendritic spines. Science 319:1683–1687. https://doi.org/10.1126/science.1152864

Toda S, Shen H, Kalivas PW (2010) Inhibition of actin polymerization prevents cocaine-induced changes in spine morphology in the nucleus accumbens. Neurotox Res 18:410–415. https://doi.org/10.1007/s12640-010-9193-z

Trantham-Davidson H, Centanni SW, Garr SC, New NN, Mulholland PJ, Gass JT, Glover EJ, Floresco SB, Crews FT, Krishnan HR, Pandey SC, Chandler LJ (2017) Binge-like alcohol exposure during adolescence disrupts dopaminergic neurotransmission in the adult prelimbic cortex. Neuropsychopharmacology 42:1024–1036. https://doi.org/10.1038/npp.2016.190

Vissavajjhala P, Janssen WG, Hu Y, Gazzaley AH, Moran T, Hof PR, Morrison JH (1996) Synaptic distribution of the AMPA-GluR2 subunit and its colocalization with calcium-binding proteins in rat cerebral cortex: an immunohistochemical study using a GluR2-specific monoclonal antibody. Exp Neurol 142:296–312. https://doi.org/10.1006/exnr.1996.0199

Whitfield TW Jr, Shi X, Sun WL, McGinty JF (2011) The suppressive effect of an intra-prefrontal cortical infusion of BDNF on cocaine-seeking is Trk receptor and extracellular signal-regulated protein kinase mitogen-activated protein kinase dependent. J Neurosci 31:834–842. https://doi.org/10.1523/JNEUROSCI.4986-10.2011

Yiu AP, Mercaldo V, Yan C, Richards B, Rashid AJ, Hsiang HL, Pressey J, Mahadevan V, Tran MM, Kushner SA, Woodin MA, Frankland PW, Josselyn SA (2014) Neurons are recruited to a memory trace based on relative neuronal excitability immediately before training. Neuron 83:722–735. https://doi.org/10.1016/j.neuron.2014.07.017